

## Stabilization of ubiquitous mitochondrial creatine kinase preprotein by APP family proteins

Xiaofan Li,<sup>a</sup> Tanja Bürklen,<sup>b</sup> Xianglin Yuan,<sup>c,d</sup> Uwe Schlattner,<sup>b</sup> Dominic M. Desiderio,<sup>c,d,e</sup> Theo Wallimann,<sup>b</sup> and Ramin Homayouni<sup>c,\*</sup>

<sup>a</sup>Department of Anatomy and Neurobiology, University of Tennessee Health Science Center, Memphis, TN 38163, USA

<sup>b</sup>Institute of Cell Biology, Swiss Federal Institute of Technology (ETH Zurich), Honggerberg HPM, Zurich, Switzerland

<sup>c</sup>Department of Neurology, University of Tennessee Health Science Center, 855 Monroe Ave, Rm 416 Link, Memphis, TN 38163, USA

<sup>d</sup>Charles B. Stout Neuroscience Mass Spectrometry Laboratory, University of Tennessee Health Science Center, Memphis, TN 38163, USA

<sup>e</sup>Department of Molecular Sciences, University of Tennessee Health Science Center, Memphis, TN 38163, USA

Received 23 April 2005; revised 6 August 2005; accepted 22 September 2005

Available online 2 November 2005

**Amyloid precursor protein (APP) is involved in the pathogenesis of Alzheimer's disease (AD). However, the physiological role of APP and its family members is still unclear. To gain insights into APP function, we used a proteomic approach to identify APP interacting proteins. We report here for the first time a direct interaction between the C-terminal region of APP family proteins and ubiquitous mitochondrial creatine kinase (uMtCK). This interaction was confirmed *in vitro* as well as in cultured cells and in brain. Interestingly, expression of full-length and C-terminal domain of APP family proteins stabilized uMtCK preprotein in cultured cells. Our data suggest that APP may regulate cellular energy levels and mitochondrial function via a direct interaction and stabilization of uMtCK.**

© 2005 Elsevier Inc. All rights reserved.

### Introduction

Amyloid precursor protein (APP), a type I transmembrane protein, is intimately involved in AD pathogenesis (Selkoe, 2000). In addition to a role in AD pathogenesis, several lines of evidence indicate that APP has important biological functions (De Strooper and Annaert, 2000; Turner et al., 2003). APP belongs to a gene family that is highly conserved throughout evolution. In mammals, there are three APP family members, including amyloid precursor like protein-1 and -2 (APLP1 and APLP2). Whereas mice with targeted disruption of the APP gene display subtle abnormalities (Zheng et al., 1995; Steinbach et al., 1998), disruption of a combination of APLP1 and APLP2 or APP and APLP2 results in perinatal lethality (von Koch et al., 1997; Heber et al., 2000).

These results suggest that the APP family members have essential and redundant roles during development. Importantly, whereas the large extracellular domain of APP family proteins is quite variable in sequence, their intracellular domains are highly conserved, suggesting that APP family proteins may participate in similar intracellular signaling pathways.

Some clues into the cellular function of APP have come from identification of APP interacting proteins (King and Scott Turner, 2004). Different regions in the cytoplasmic tail of APP have been shown to bind to heterotrimeric G $\alpha$  protein (an intracellular signal transducer) (Nishimoto et al., 1993), kinesin light chain (axonal transport protein) (Kamal et al., 2000, 2001), or PAT1 (a microtubule-associated protein) (Nishimoto et al., 1993; Zheng et al., 1998; Kamal et al., 2000, 2001). In addition, the C-terminal region of APP family proteins, containing the amino acid sequence motif NPxY, interacts with the phosphotyrosine-binding (PTB) domain of a number of intracellular adapter proteins such as Dab1, X11, and Fe65, which are involved in distinct cellular processes (Homayouni et al., 1999; Kimberly et al., 2001; King et al., 2003). Notably, most of these interactions were identified by yeast two-hybrid approaches that only detect one-to-one protein interactions in an artificial yeast nuclear environment. Thus, alternative approaches are necessary to identify multi-protein complexes or APP interactions that require specific cellular environments or post-translational modifications. For instance, using a biochemical approach, Zhou et al. (2004) recently identified a novel interaction between tyrosine-phosphorylated APP cytoplasmic domain and growth factor receptor-bound protein 2 (Grb2) (Zhou et al., 2004). In addition, Ho and Sudhof used a functional proteomic approach to identify F-spondin as a novel extracellular ligand of APP (Ho and Sudhof, 2004).

We hypothesize that the C-terminal regions of APP family proteins engage in similar intracellular functions through interactions with multi-protein complexes. Therefore, we used a

\* Corresponding author. Fax: +1 901 448 7440.

E-mail address: rhomayouni@utmem.edu (R. Homayouni).

Available online on ScienceDirect (www.sciencedirect.com).

functional proteomic strategy, involving biochemical affinity chromatography and peptide mass fingerprinting, to identify new APP interacting proteins. Here, we report identification of ubiquitous mitochondrial creatine kinase (uMtCK, EC 2.7.3.2) with the C-terminal region of APP family proteins. This association was confirmed by surface plasmon resonance spectroscopy *in vitro* and by co-immunoprecipitation (co-IP) from cell culture and brain extracts. The interaction of APP with uMtCK stabilized the immature form of uMtCK in cultured cells. Creatine kinase (CK) catalyzes the reversible transfer of high energy phosphate from ATP to creatine, yielding phosphocreatine for energy storage and transport (Wallimann et al., 1992). There are several isoenzymes of CK with distinct tissue and cellular distributions. In the brain, the cytosolic brain-type CK (BCK) and uMtCK comprise an energy shuttling system, which transfers energy efficiently from the site of ATP production (mitochondria) to distal parts of the cell where energy is consumed (Wallimann et al., 1998; Joubert et al., 2002). In addition, uMtCK may affect mitochondrial transport and ionic homeostasis by forming a high energy channeling complex consisting of porin and adenine nucleotide translocator (ANT) (Dolder et al., 2001; Schlattner et al., 2001). Taken together, our studies suggest a new role for APP in modulation of uMtCK levels and possibly cellular energy metabolism.

## Results

### Identification of ubiquitous mitochondrial creatine kinase as an APLP1 interacting protein

To identify protein complexes associated with cytoplasmic domain of APP proteins, we used a functional proteomic approach. Mouse brain homogenates were passed through columns containing sepharose beads cross-linked with synthetic peptide (A1 peptide) corresponding to the last 18 amino acids of APLP1 cytoplasmic domain, which is highly conserved among the APP family proteins (Homayouni et al., 1999). After extensive washing, the bound proteins were eluted and subjected to 1-D or 2-D electrophoresis and silver staining. We identified a number of proteins that preferentially bound to A1 peptide, and not to the randomized control peptide, by tryptic peptide fingerprinting using MALDI-TOF spectrometry (data not shown). Among these proteins were several subunits of adapter-related protein complex AP-2, which are known to bind to NPxY-containing sequences and are necessary for clathrin-mediated endocytosis (Bonifacino and Traub, 2003). Another protein that preferentially bound to the A1 peptide was identified as uMtCK (NP\_034027) (Figs. 1A and B).

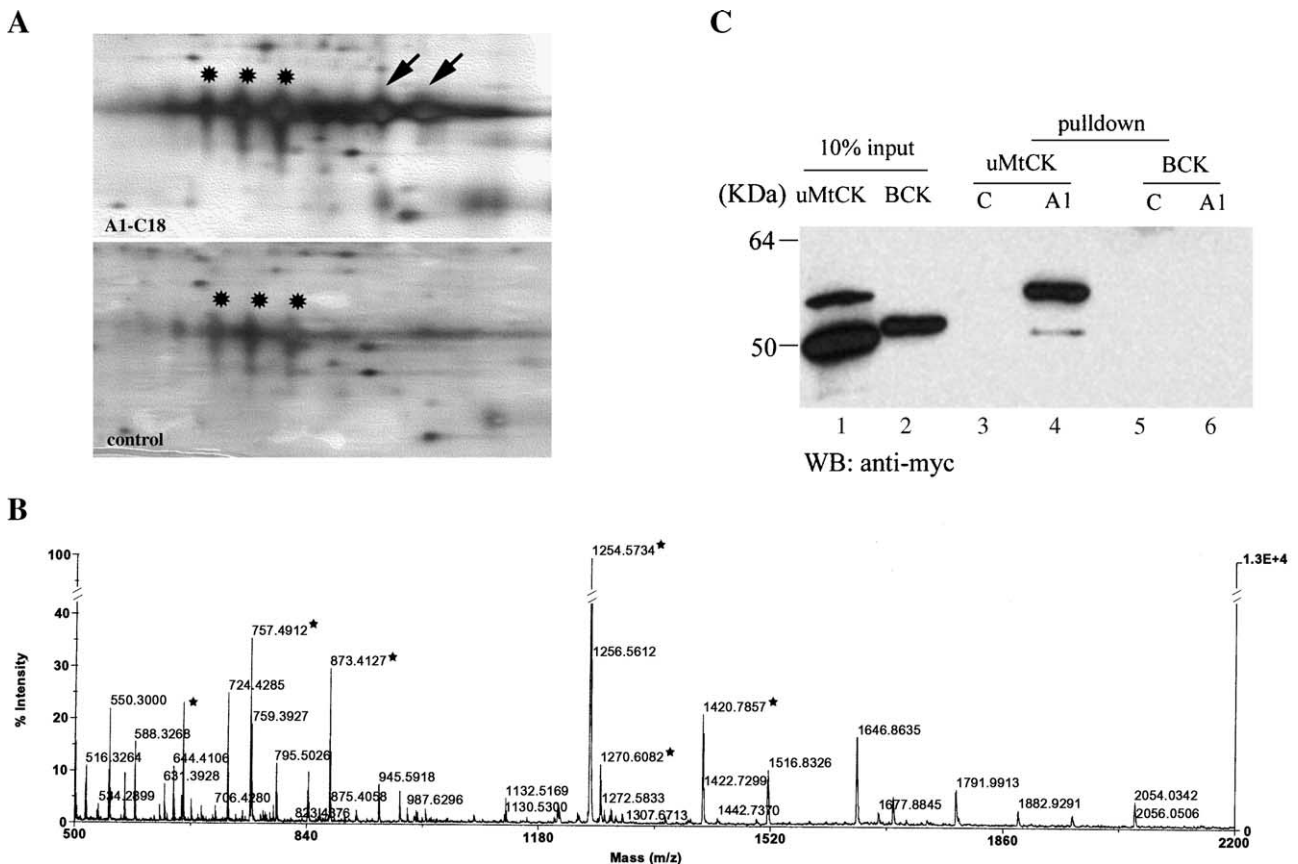


Fig. 1. Identification of ubiquitous mitochondrial creatine kinase as a novel APLP1 interacting protein. (A) 2-D gel images of proteins that bound to A1 peptide (top panel) compared with control peptide (bottom panel). Two proteins that preferentially bound to the A1 peptide (arrows) were excised from the gel and processed for tryptic peptide fingerprinting. Stars indicate proteins that non-specifically bound to the control peptide. (B) Mass spectra of peptides obtained from the proteins denoted by arrows in panel (A). Stars indicate the peptides that corresponded to uMtCK. (C) Confirmation of uMtCK–A1 interaction by biochemical pull-down experiments. Lysates from COS7 cells transiently transfected with either uMtCK-myc or BCK-myc were incubated with either A1 peptide (A1, lanes 4 and 6) or control randomized peptide (C, lanes 3 and 5) immobilized to sepharose beads. The protein complexes were separated by SDS-PAGE and examined by Western blotting using anti-myc antibodies. As a control, 10% of input lysates were also loaded on the gels (lanes 1–2).

To confirm the interaction between uMtCK and A1 peptide, we performed biochemical pull-down experiments using cell lysates transiently transfected with either mitochondrial uMtCK-myc or cytosolic BCK-myc constructs. Fig. 1C shows that A1 peptide specifically interacted with uMtCK-myc but not with BCK-myc. Interestingly, a higher molecular weight band of uMtCK-myc seemed to preferentially bind to the A1 peptide.

Since biochemical affinity experiments can identify multi-protein complexes, we tested whether the interaction of A1 peptide with uMtCK is direct or indirect by using surface plasmon resonance (SPR) spectroscopy. The association and dissociation kinetics of A1 peptide binding to purified recombinant BCK or uMtCK was determined in ‘physiological’ buffer conditions (0.1% Triton, 100 mM NaCl). Consistent with the pull-down experiments above, we found that uMtCK bound preferentially to A1 peptide as compared to the random peptide (Figs. 2A and B), while cytosolic BCK bound neither peptide (Figs. 2C and D). Because the uMtCK–A1 interaction showed a very fast association rate (Fig. 2B), a direct fit of the kinetics was impossible. However, Scatchard plot analysis revealed an affinity of  $175 \pm 30$  nM for the A1 peptide, as compared to  $430 \pm 115$  nM for the low level binding to random peptide. These data demonstrate that interaction of A1 peptide with uMtCK is direct and of rather high affinity. Given the fact that A1 and the control peptide have identical amino acid compositions, the differences in their binding properties obtained under these conditions are considerable.

#### *uMtCK associates with full-length APLP1 and C-terminal fragment of APP in cultured cells*

To examine whether full-length APLP1 and uMtCK interact in cells, we carried out co-immunoprecipitation experiments using transiently transfected COS7 cells. We found an association between uMtCK-myc and APLP1-flag in both uMtCK and APLP1 immunoprecipitates (Figs. 3A and B). Consistent with our earlier results, we found that only the large molecular weight form of uMtCK-myc associated with full-length APLP1 in COS7 cells.

APP family proteins can be proteolytically cleaved by secretases and caspases, which lead to intracellular release of their cytoplasmic domains (Galvan et al., 2002; Scheinfeld et al., 2002; Eggert et al., 2004). Therefore, we tested if the soluble intracellular domain of APP also interacts with uMtCK. Co-immunoprecipitation experiments were performed using lysates from COS7 cells which were transiently transfected with uMtCK-myc and an eGFP fusion construct containing the C-terminal 31 amino acids in APP (eGFP-APP-C31). We found that eGFP-APP-C31 strongly associated with uMtCK (Fig. 3C).

To investigate the subcellular site of interaction between APP and uMtCK, we performed laser confocal microscopy on COS7 cells transiently transfected with uMtCK-myc along with either full-length APLP1-flag or eGFP-APP-C31 (Figs. 3D and E). As expected, uMtCK staining was observed in irregular structures resembling mitochondria around the nucleus and throughout the cytoplasm. Similar structures were observed using the mitochon-

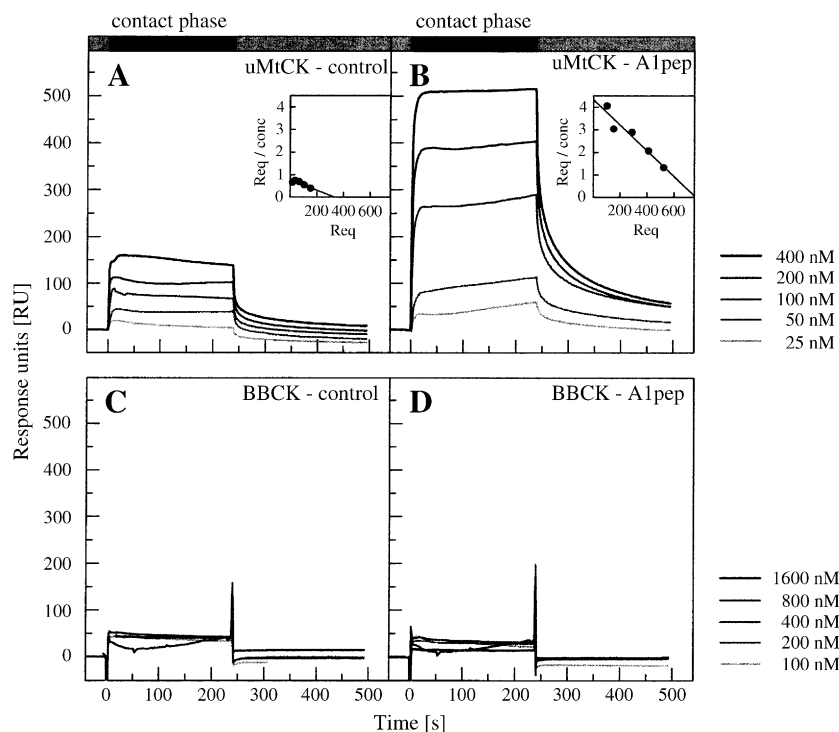


Fig. 2. Interaction of uMtCK and APLP1 peptide is direct, specific, and of high affinity. Representative SPR traces of contact and dissociation phase of human uMtCK (A, B) or human BCK (C, D) with randomized control peptide (A, C) or specific APLP1 peptide (B, D). Representative traces for 25, 50, 100, 200, and 400 nM octameric uMtCK and 100, 200, 400, 800, and 1600 nM dimeric BCK are shown. (Inserts in panels A and B) Scatchard plots derived from the relationship between octamer concentration (*conc*, in nM) and SPR signal at equilibrium (*Req*, in RU) to estimate affinity  $K_D$ . SPR data were recorded at 25°C and a flow rate of  $1.2 \text{ ml h}^{-1}$  with 50 mM TES pH 7.4, 100 mM NaCl, and 0.1% Triton X-100 as running buffer. Response units (RU) are proportional to the amount of bound CK.

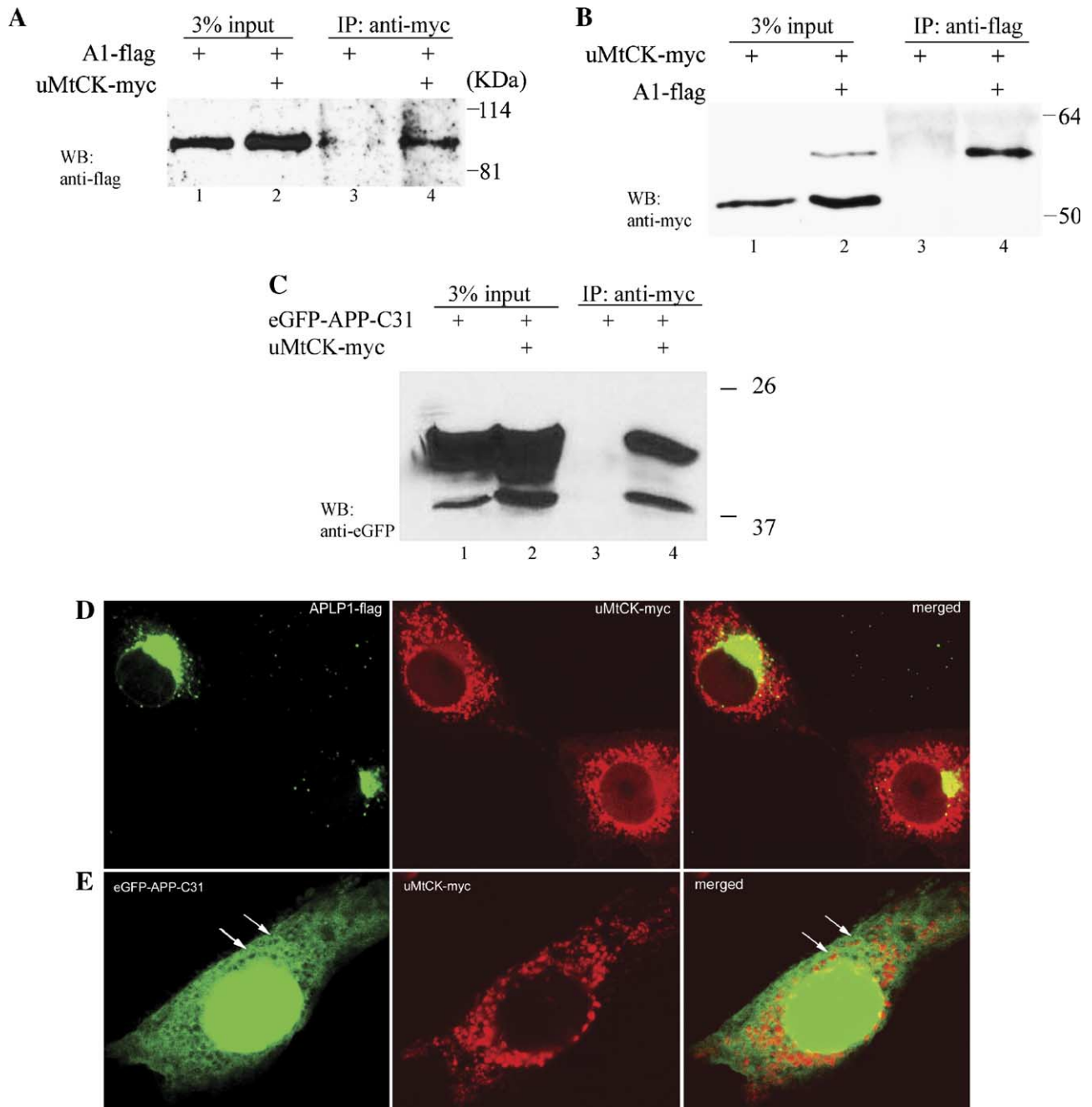


Fig. 3. uMtCK interacts with full-length APLP1 in cultured cells. (A) Protein lysates from COS7 cells transfected with APLP1-flag alone (lane 3) or APLP1-flag plus uMtCK-myc (lane 4) constructs were immunoprecipitated with anti-myc and immunoblotted with anti-flag antibodies. (B) Protein lysates from COS7 cells transfected with uMtCK-myc alone (lane 3) or uMtCK-myc plus APLP1-flag (lane 4) constructs were immunoprecipitated with anti-flag and immunoblotted with anti-myc antibodies. (C) Protein lysates from COS7 cells transfected with eGFP-APP-C31 alone (lane 3) or eGFP-APP-C31 plus uMtCK-myc (lane 4) constructs were immunoprecipitated with anti-myc antibody and immunoblotted with anti-eGFP antibodies. As a control, 3% of input lysates were loaded on the gels (lanes 1 and 2, A–C). (D) COS7 cells were transfected with APLP1-flag and uMtCK-myc. Subcellular localization of APLP1-flag and uMtCK-myc was examined by immunofluorescence using laser confocal microscopy. APLP1-flag was visualized using anti-APLP1 polyclonal antiserum (CT11) and Alexa 480-red conjugated anti-rabbit antibody (green fluorescence, left panel), and uMtCK-myc was visualized using monoclonal anti-myc antibody and Alexa 594-conjugated anti-mouse antibody (red fluorescence, middle panel). A merged image is shown in the right panel. (E) COS7 cells were transfected with eGFP-APP-C31 and uMtCK-myc. Subcellular localization of eGFP-APP-C31 and uMtCK-myc was examined by immunofluorescence using laser confocal microscopy. eGFP-APP-C31 is shown in green fluorescence (left panel), and uMtCK-myc was visualized using monoclonal anti-myc antibody and Alexa 594-conjugated anti-mouse antibody (red fluorescence, middle panel). A merged image is shown in the right panel. Arrows mark the honeycomb staining pattern observed for eGFP-APP-C31 protein due to its absence in the mitochondria, marked uMtCK staining.

drial marker MitoTracker (Molecular Probes) in COS7 cells (Data not shown). On the other hand, APLP1 staining was observed primarily in the ER/Golgi and in smaller vesicular structures throughout the cytoplasm. Very little overlap in staining was observed between uMtCK and APLP1 staining. This result suggests that APLP1 is not targeted to mitochondria, the predominant site of uMtCK protein. However, it is possible that the interaction of the cytosolic uMtCK preprotein with APLP1 occurs in the ER/Golgi at concentrations that are below detection in this assay. In contrast to APLP1-myc, eGFP-APP-C31 fluorescence was intense in the nucleus and diffuse throughout the cytoplasm (Figs. 3D and E). Interestingly, the eGFP-APP-C31 staining was absent in the mitochondria and more pronounced around the mitochondria in the perinuclear region, resulting in a honeycomb-like staining pattern.

#### *uMtCK associates with all three APP family members in brain*

To determine whether the interaction between uMtCK and APP family proteins occurs in physiological conditions, we performed co-IP experiments using brain homogenates. uMtCK was immunoprecipitated from adult mouse brain homogenates using anti-human uMtCK (anti-huMtCK) antiserum. The protein complexes were stringently washed with RIPA buffer and then examined by SDS-PAGE and Western blotting using anti-APP, anti-APLP1, or anti-APLP2 antibodies. We found that anti-huMtCK antiserum, but not the pre-immune serum, precipitated all three APP family members (Fig. 4A). Interestingly, only the lower molecular weight forms, presumably the immature unglycosylated forms (Lyckman et al., 1998), of APP and APLP2 associated with uMtCK. In addition, using confocal laser microscopy on cultured cortical neurons, we found that APP co-localizes with uMtCK predominantly in the perinuclear region, although some co-localization was also observed along the processes (Fig. 4B). Co-localization of APP and uMtCK in

neurons is different from our observations in COS7 cells (above) and may account for the high efficiency of the co-IP in brain (Fig. 4A) as compared to COS7 cells (Figs. 3A and B). Taken together, these data suggest that interaction of uMtCK and APP family proteins can occur under physiological conditions in the brain.

#### *Stabilization of uMtCK preprotein by APP family proteins*

During the co-IP experiments, we observed that the steady state level of the higher molecular weight form of uMtCK (HMr-uMtCK) was increased by co-transfection of all three family members of APP using cultured COS7 cells (data not shown). We investigated this phenomenon further in a new series of experiments. We found that expression of full-length APLP1-flag or eGFP-APP-C31 protein led to an accumulation of HMr-uMtCK (Fig. 5A). These effects were specific since co-transfection of very low density lipoprotein receptor (VLDLR), another transmembrane protein containing a cytoplasmic NPxY sequence, did not increase the HMr-uMtCK. In addition, the effect of eGFP-APP-C31 was concentration-dependent as increasing amounts of eGFP-APP-C31 produced more HMr-uMtCK (Fig. 5B). Notably, the lower Mr form of uMtCK was also increased, especially under the lower amount of eGFP-APP-C31 when the accumulation of HMr-uMtCK was not so dramatic.

uMtCK is highly susceptible to oxidative damage (Wendt et al., 2003). Thus, one possibility is that transfection of APP proteins increases oxidative stress, resulting in a modification of uMtCK that retards its migration in SDS gels. On the other hand, APP proteins may stabilize the immature unprocessed form of uMtCK, which contains an N-terminal mitochondrial targeting sequence. Therefore, we set out to identify the HMr-uMtCK that accumulated after APP co-expression. First, the higher molecular weight form of uMtCK appeared to be approximately 5 kDa larger than expected. This is consistent with the calculated Mr of the 39 amino acid

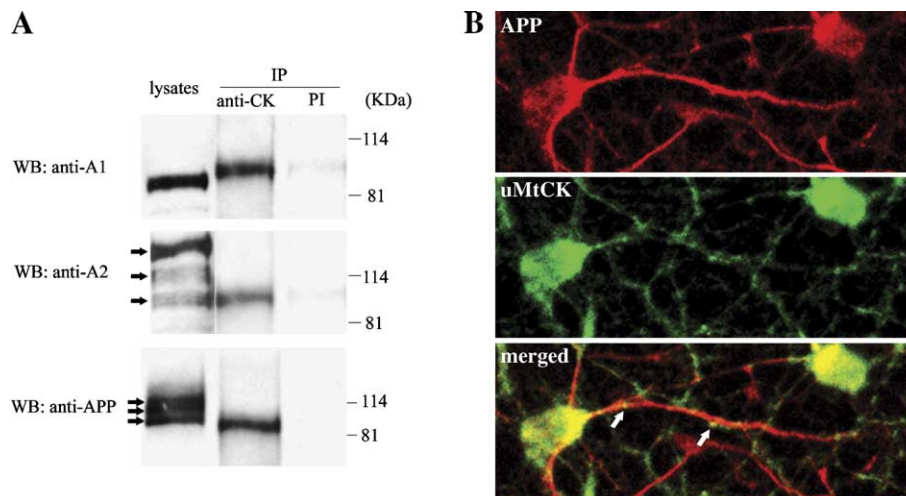


Fig. 4. uMtCK interacts with APP family proteins in brain. (A) Approximately 200  $\mu$ g of total protein from mouse brain homogenates was immunoprecipitated with either anti-huMtCK antiserum (anti-CK) or the pre-immune serum (PI). Protein complexes were washed in RIPA buffer and examined by immunoblotting using anti-APLP1 (top panel), anti-APLP2 (middle panel), and anti-APP (bottom panel) antibodies. Approximately 20  $\mu$ g of total protein was loaded on the gel as control (lysate). Arrows indicate multiple forms of APLP2 and APP, presumably due to glycosylation. (B) Subcellular localization of uMtCK and APP in primary neuronal cultures (4 days in vitro) was examined by immunofluorescence using laser confocal microscopy. APP was visualized using anti-APP monoclonal antiserum (22C11) and Texas-red-conjugated anti-mouse antibodies (top panel), and uMtCK was visualized using rabbit anti-human uMtCK and FITC-conjugated anti-rabbit antiserum (middle panel). A merged image is shown in the bottom panel to better illustrate the subcellular co-localization (yellow). Arrows point to punctate staining along the neuronal processes.

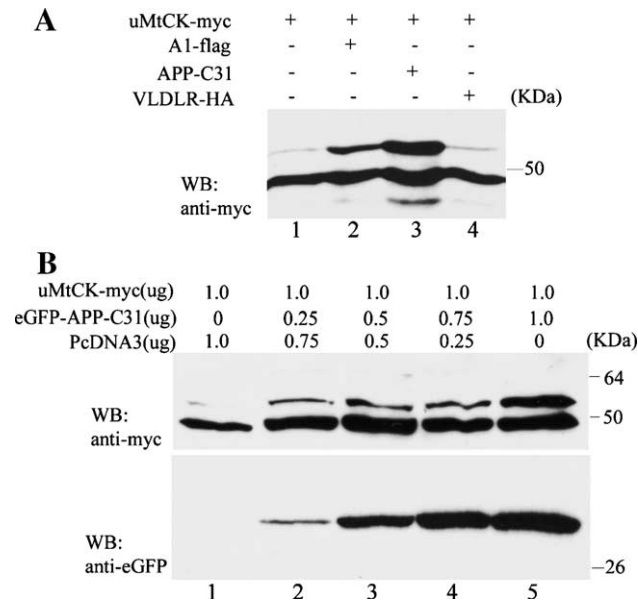


Fig. 5. Stabilization of high molecular weight (HMr) uMtCK by APP family proteins. (A) Immunoblotting was performed using anti-myc antibody on 30  $\mu$ g of total protein prepared from COS7 cells transfected with uMtCK-myc alone (lane 1) or co-transfected with APLP1-flag (lane 2), eGFP-APP-C31 (lane 3), or VLDLR-HA (lane 4). (B) Immunoblotting was performed using anti-myc (top panel) or anti-eGFP (bottom panel) on COS7 cells transfected with uMtCK-myc alone (lane 1) or along with increasing amounts of eGFP-APP-C31 construct (lanes 2–5).

residues leader sequence, which is cleaved after its mitochondrial targeting. In crude fractionation experiments, we found that the HMr-uMtCK was not associated with the mitochondria, whereas the lower uMtCK band was enriched in the mitochondrial fraction (Fig. 6A). We next examined the turnover rate and degradation of the two uMtCK bands by performing pulse chase analysis (Fig. 6B). We found that both bands were labeled with [ $^{35}$ S]-Met/Cys immediately after the 8-min labeling period. Within 2 h after the labeling period, the upper band was decreased substantially, while the lower band persisted. This is consistent with the notion that the upper band is the pre-processed form of uMtCK that is rapidly converted into the more stable mature mitochondrial form after cleavage of the signal sequence. When cells were co-transfected with eGFP-APP-C31, both upper and lower bands of uMtCK were increased. If indeed the HMr-uMtCK were derived from oxidative or post-translational modification of the mature uMtCK form, we would expect to see a decrease in the amount of the lower band in proportion to an increase in the amount of the upper band. Thus, our results suggest that APP stabilizes the uMtCK preprotein. Lastly, we examined whether the HMr-uMtCK contained the signal sequence using electrospray tandem mass spectrometry. COS7 cells were transiently transfected with uMtCK-myc and eGFP-APP-C31 to enrich the HMr-uMtCK band and then processed for A1 affinity binding as described above. Two bands (~Mr 47 and 52 kDa) were excised from gels and digested with trypsin. The resulting peptides were separated by LC/MS and sequenced by electrospray mass spectrometry. Both bands were identified as uMtCK, however, only the upper band contained a peptide

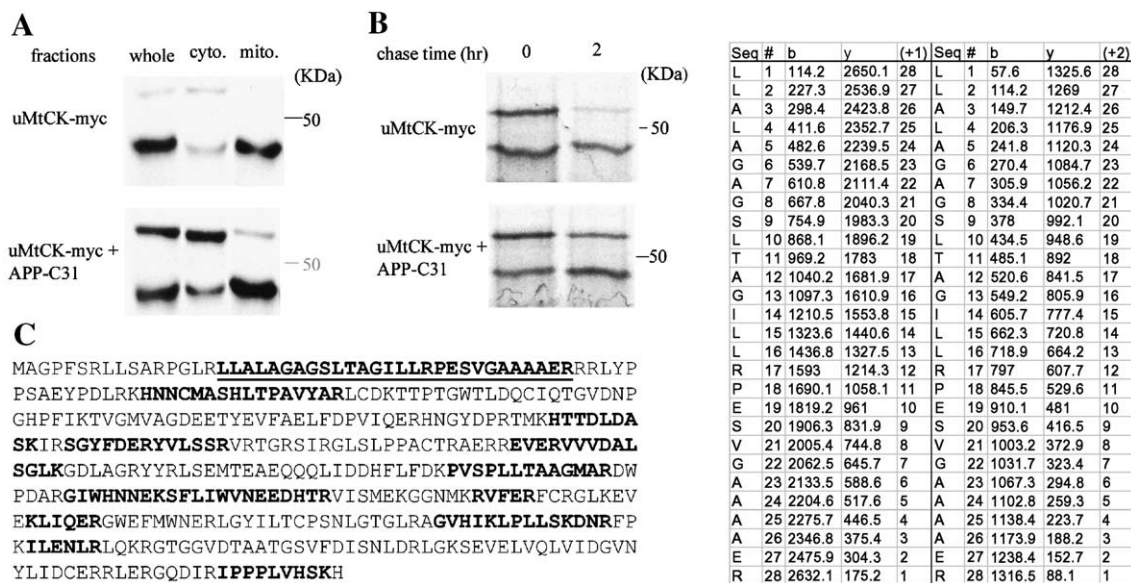


Fig. 6. Identification of the high Mr band of uMtCK as uMtCK preprotein. (A) Differential centrifugation was performed on COS7 cells transfected with uMtCK-myc alone (upper panel) or along with eGFP-APP-C31 (lower panel). uMtCK was detected by immunoblotting using anti-myc antibodies on whole lysate (whole), cytosolic (cyto.), and mitochondria-enriched fractions (mito.). (B) COS7 cells transfected with uMtCK-myc alone (upper panel) or along with eGFP-APP-C31 (lower panel) were metabolically labeled with  $^{35}$ S-Met/Cyst for 8 min and then chased with cold medium for 2 h. uMtCK was immunoprecipitated using anti-myc antibodies, separated by SDS-PAGE, and visualized by autoradiography. (C) The high Mr band observed in COS7 lysates transfected with uMtCK-myc and eGFP-APP-C31 was excised from a SDS gel, trypsinized, and then subjected to electrospray tandem mass spectrometry. We identified and sequenced 18 peptides covering 36.8% of uMtCK protein sequence (in bold, left panel). The sequence of one peptide (right panel) corresponded to the N-terminal signal sequence in uMtCK (underlined, left panel). Arrow in left panel indicates the predicted cleavage site of uMtCK signal sequence. The right panel shows the theoretical masses of b- and y-fragment ions of this peptide. The detection of continuous y-ion series and b-ion series (shaded) confirms the amino acid sequence of this peptide.

containing the signal sequence for uMtCK (Fig. 6C). Taken together, these results indicate that the high molecular weight form of uMtCK, which is stabilized by APP, is indeed uMtCK preprotein and not an oxidative derivative.

## Discussion

In this study, we show that uMtCK interacts with APP family proteins in cultured cells as well as in the brain using co-immunoprecipitation assays. This interaction is direct and of high affinity as shown by surface plasmon resonance experiments. Importantly, we found that overexpression of APP cytoplasmic domain in cultured cells stabilized a higher molecular weight form of uMtCK, which we identified as the uMtCK preprotein containing the mitochondrial targeting sequence.

uMtCK is encoded by the nuclear genome, synthesized by ribosomes, and then translocated to mitochondria via its N-terminal signal sequence. In the mitochondria, uMtCK dimers or octamers are localized in the cristae and the intermembrane space (contact sites) of mitochondria (Schlattner et al., 1998). It is likely that mitochondrial targeting of uMtCK involves cytosolic chaperones such as mitochondria-import stimulating factor (MSF) or arylhydrocarbon receptor-interacting protein (AIP) (Mihara and Omura, 1996; Yano et al., 2003) as well as the translocase of outer mitochondrial membrane (TOM) protein family (Pfanner and Wiedemann, 2002). Mitochondrial chaperones assist in the import of mitochondrial proteins by directly binding to the preprotein and preventing their aggregation, misfolding, and proteolysis. Overexpression of mitochondrial chaperone proteins in cultured cells has been shown to stabilize mitochondrial preproteins (Yano et al., 1998). Consistent with these observations, we found that APP C31 expression decreased the turnover and increased steady state levels of uMtCK preprotein. Indeed, we have found that overexpression of full-length APLP1 in HEK293T cells results in an increase in dimeric and octameric CK activity (Bürklen and Wallimann, unpublished observations). These results suggest that APP may function as a cytosolic chaperone for uMtCK preprotein and consequently increase CK activity and cellular energy metabolism.

The hypothesis that APP may function as a chaperone protein was proposed over 10 years ago by Liautard (1994). APP is known to be an acute phase response gene induced by cellular stress and neuronal injury. For example, APP expression is induced together with several stress response proteins such as C-FOS and heat shock protein 70 after cerebral ischemia (Hall et al., 1995; Lin et al., 1999). Since ischemia is an energy deficiency insult, it is reasonable to assume that neurons would respond by stabilizing enzymes that are critical for production and maintenance of energy. Indeed, APP has been shown to play a neuroprotective role against other insults in neurons. For example, Kogel et al. (2003) recently demonstrated that APP, but not APP<sub>swc</sub>, protects PC12 cells against the unfolded protein response induced by prolonged treatments with inhibitors of glycosylation (tunicamycin) or ER-to-Golgi transport (brefeldin A) (Kogel et al., 2003).

Accumulating evidence suggest that mitochondria play a central role in neurodegeneration as well as AD through modulation of cellular energy, calcium levels, and reactive oxygen species (Swerdlow and Khan, 2004). An alternative hypothesis has been proposed for late-onset AD, which states that neurodegeneration in AD results from mitochondria genome deficits which lead to accumulation of damage caused by reactive oxygen species

(Mattson, 1997; Swerdlow and Khan, 2004). There is mitochondrial dysfunction and increased oxidative stress in AD brains (Smith et al., 1991; Gibson et al., 1998; Eckert et al., 2003). Positron emission tomography studies showed reduced brain glucose utilization in early stages of AD brain (Rapoport et al., 1996). In addition, a group of genes involved in mitochondrial metabolism were up-regulated in the early stage of pathological changes in the APP transgenic mouse model (Reddy et al., 2004). Together, these findings point to a close link between mitochondria and early pathogenesis of AD. However, the precise role that APP plays in this model is not clear. An N-terminal sequence in APP was shown to target APP to mitochondria in a membrane arrested form and cause disruption of mitochondrial metabolism (Anandatheerthavarada et al., 2003). In contrast, we did not observe a significant targeting of full-length APLP1 or APP C-terminal fragment to mitochondria (Figs. 3D and E).

uMtCK has been shown to be important to mitochondrial function in several ways. It has a protective role against oxidative or toxic insults to the mitochondria (O’Gorman et al., 1997; Kanazawa et al., 1998; Dolder et al., 2003; Hatano et al., 2004). uMtCK is also important for mitochondrial energy channeling (Wallimann et al., 1992, 1998) and permeability transition (O’Gorman et al., 1997; Dolder et al., 2003). Interestingly, the fact that transgenic ablation of uMtCK leads to impaired learning and memory in mice (Streijger et al., 2004) suggests that uMtCK may play a role in cognitive deficits such as in AD. Therefore, the identification of a direct interaction between APP and uMtCK may provide important insights not only into the physiological roles of APP family proteins but also on the pathological roles of APP in the neurodegeneration associated with AD.

## Experimental methods

### Materials

A1 (CELQRHGYENPTYRFLLEE) peptide and control randomized peptide (CFEYRNRHQETPELLGET) were described previously (Homayouni et al., 1999). The antibodies used in this study were anti-myc (Invitrogen Life Technologies), anti-eGFP (Invitrogen Life Technologies), anti-flag (clone M2, Sigma-Aldrich), anti-APP-Cterm (Sigma-Aldrich), anti-APLP1 (CT11, Calbiochem), anti-APLP2 (CT12, Calbiochem) and anti-huMtCK described in Schlattner et al. (2002). CK isoenzymes were expressed in *E. coli* and purified as described in Schlattner et al. (2000).

### Plasmid construction

Several expression constructs used in this study were described previously: PcDNA3-VLDLR-HA by D’Arcangelo et al. (1999) PcDNA3-mAPP695 and PcDNA3-mAPLP1 by Homayouni et al. (1999). PcDNA3-APLP1-flag was generated by inserting the full-length mouse APLP1 cDNA (Homayouni et al., 1999) into PcDNA3-flag construct described in Homayouni et al. (2001). pCS<sup>2+</sup>-eGFP fusion constructs containing APP-C31 were generated by PCR amplification using nested *EcoRI* and *XbaI* primers and the full-length PcDNA3-APP as template. PcDNA3-uMtCK-myc and PcDNA3-BCK-myc constructs were made by reverse transcription PCR using wild type mouse brain RNA library. All PCR products were confirmed by sequencing. Primers used for these constructs are listed in Supplementary Table 1.

### Affinity binding and 2-D electrophoresis

Synthetic A1 and control peptides were cross-linked to agarose resin using SulfoLink kit (Pierce, USA) and packed into 1 ml columns. Wild type mice brains were homogenized in brain homogenization buffer (50 mM Tris–HCl, 1% Triton X-100, 5% glycerol, 150 mM NaCl, 2  $\mu$ M leupeptin, and aprotinin) and pre-cleared by centrifugation at  $20,000\times g$  for 30 min. The supernatants were passed through the columns and washed extensively with brain homogenization buffer. After a final wash with 50 mM Tris–HCl, the bound proteins were eluted with rehydration solution (7 M urea, 2 M thiourea, 4% CHAPS, 0.8% IPG buffer and trace of bromophenol blue) supplemented with DTT and loaded onto pH3-10L strip (Amersham Pharmacia Biotech). Isoelectric focusing electrophoresis (IEF) was performed in IPGphor (Amersham Pharmacia Biotech) followed by the second dimension SDS-PAGE on the protean II cell following manufacturer's protocols (Bio-Rad laboratories). Proteins were visualized by silver staining as described by Yuan et al. (2002).

### Peptide fingerprinting by MALDI-TOF mass spectrometry

Gel pieces were minced, de-stained, and digested with trypsin (Promega, WI) overnight at 37°C. The tryptic peptides were extracted with 60% acetonitrile/5% TFA by sonication. The peptide mixture was purified by Ziptip C18 (Millipore, MA) and eluted directly onto the MALDI plate with  $\alpha$ -cyano-4-hydroxycinnamic acid (CHCA) solution in 50% acetonitrile/0.1% TFA. The MALDI spectra were collected using a Voyager DE-RP mass spectrometer (Framingham, MA) in the delayed extraction and reflector mode with internal calibration of trypsin autolysis products. The unique peaks in the spectra from one gel spot were compared to the tryptic peptide patterns of proteins in the non-redundant protein database at NCBI using Mass-Fit program available on the website of <http://prospector.ucsf.edu>.

### Liquid chromatography mass spectrometry (LC-MS)

These methods were described in detail previously by Yuan and Desiderio (2003). Samples were prepared as described above. Tryptic peptides extracted in 60% acetonitrile/5% TFA were concentrated by vacuum centrifugation and dissolved in 0.1% formic acid followed by separation with homemade on-line HPLC column (10 cm in length; i.d. 75  $\mu$ m; packing material: C18, 200  $\text{\AA}$ ) and then were sequenced with nano-ESI method using an LCQ<sup>deca</sup> LC-ESI-Q-IT MS instrument (ThermoFinnigan, CA). LCQ sequence data were used to query the SWISS-PROT database using the SEQUEST program.

### Surface plasmon resonance (SPR) spectroscopy

The interaction of A1 and random peptides with CK isoforms was analyzed by surface plasmon resonance (SPR) with a Biacore 2000™ instrument (Biacore, Uppsala). Peptides were dissolved in 10 mM Na–citrate pH 4.5 to a concentration of 0.05 mg/ml. About 300 RU peptide per lane (400 fmol/mm<sup>2</sup>) was immobilized by thiol disulfide exchange between their C-terminal cysteines and PDEA that was previously coupled to the carboxydextran surface of CM5 sensorchips according to the supplier's instructions (PDEA thiol coupling kit, Biacore, Uppsala). Excess reactive groups were deactivated by 50 mM cysteine in 1 M NaCl. CK protein stocks

were exchanged against running buffer (50 mM TES pH 7.4, 100 mM NaCl, 0.1% Triton X-100) via gel filtration (PD10 columns, Amersham). CK–peptide association and dissociation kinetics were recorded at 25°C in running buffer at a flow rate of 1.2 ml h<sup>-1</sup> with CK concentrations ranging from 25 to 1600 nM. The peptide surface was recovered by a final injection of 1 M NaCl. Kinetic data were corrected for background binding to the empty PDEA surface. The affinity was derived from the slope of a plot  $R_{eq}/c$  versus  $c$ , analogous to a Scatchard plot. Data are given as mean  $\pm$  standard deviation (SD).

### Cell culture and co-immunoprecipitation

COS7 cells were maintained in DMEM containing 10% FCS at 37°C in 5% CO<sub>2</sub>. Cells were transiently transfected with plasmids using FuGene 6.0 following the manufacturer's protocol (Roche, Germany). About 48 h post-transfection, the cells were harvested in lysis buffer (PBS containing 1% Triton X-100, 5% glycerol, 150 mM NaCl, and 2  $\mu$ M leupeptin, and Aprotinin). The lysates were cleared at  $20,000 \times g$  for 20 min in a microcentrifuge before incubation with primary antibody at 4°C overnight and followed by incubation with protein G–sepharose beads (Pierce Chemical Co., Rockford, IL) at 4°C for 2 h. The protein complexes were washed three times with lysis buffer, and the bound proteins were eluted with 2 $\times$  Laemmli buffer and analyzed by SDS-PAGE and Western blotting. For brain co-IP, the protein complexes were washed 3 times in RIPA buffer (150 mM NaCl, 10 mM Tris pH 7.2, 1% Triton X-100, 0.1% SDS, 1% deoxycholate, 5 mM EDTA).

### SDS-PAGE and immunoblot analysis

Proteins were resolved by SDS-PAGE and transferred to nitrocellulose membrane for immunoblot analysis. The membrane was blocked in 5% non-fat milk in TBST (263 mM NaCl, 150 mM Tris–HCl, 0.5% Tween-20, pH 7.4) at room temperature for 1 h and incubated with anti-myc antibody (1:5000), anti-huMtCK (1:2000), anti-flag M2 (1:5000), anti-APP (1:8000), anti-APLP1 (1:5000), anti-APLP2 (1:2000), or anti-EGFP (1:350). The membrane was subsequently incubated with either anti-rabbit or anti-mouse IgG–HRP-conjugated secondary antibody for another hour. Proteins were visualized using chemiluminescence Supersignal West Pico or West Femto kit (Pierce Chemical Co., Rockford, IL).

### Differential centrifugation

The crude mitochondria preparations from transfected COS7 cells were collected using Mitochondria Isolation Kit (Pierce Chemical Co., Rockford, IL) according to the manufacturer's protocol. Briefly, transfected cells were pelleted at  $1000 \times g$  for 5 min, washed with 1 $\times$  DPBS and resuspended in reagent A. After addition of reagents B and C, the supernatant was centrifuged at  $700 \times g$  and again at  $3000 \times g$  to obtain the mitochondria-enriched fraction.

### Metabolic labeling and IP

Transfected COS7 cells were starved in labeling medium (DMEM without L-Met, L-Gln, and L-Cys, 10% dialyzed FBS, 1% P/S, 2 mM Glu) for 1 h and then incubated in labeling medium containing 0.2 mCi/ml [<sup>35</sup>S]-protein labeling mix (NEG-772, Perkin-Elmer Life Sciences, Inc.) for 8 min at 37°C. Immediately after labeling, the cells were washed in normal DMEM medium. At

specific chase time points, the cells were lysed in 1% Triton lysis buffer as described above. uMtCK was immunoprecipitated using anti-myc antibody and protein G–sepharose beads at 4°C for 2 h. The immunoprecipitates were washed three times with RIPA buffer and subjected to SDS-PAGE and autoradiography.

#### Primary neuronal culture and immunocytochemistry

Embryonic day 18 mouse telencephalon was dissected, and the cells were dissociated by trituration in Hank's balanced salt solution (HBSS) without  $\text{Ca}^{2+}$  and  $\text{Mg}^{2+}$ , supplemented with 1.0 mM sodium pyruvate and 10 mM HEPES. Approximately,  $3 \times 10^6$  cells were plated on poly-D-lysine-coated coverslips in a 60 mm dish. Cells were maintained in B27 supplemented neurobasal medium for 4 days and then fixed and permeabilized in 4%PFA/0.1% Triton in  $1 \times$  PBS. After blocking in 3% horse serum at room temperature for 15 min, the cells were incubated with anti-uMtCK (1: 500) and anti-APP (1:500) in  $1 \times$  PBST for 1 h at RT, washed  $3 \times 5$  min with PBST, then incubated with FITC conjugated anti-rabbit (1:1000) and TR-conjugated anti-mouse (1:1000) for 30 min at room temperature. Fluorescence was examined by confocal laser microscopy (BIO-RAD MRC-1024, Bio-Rad laboratories).

#### Acknowledgments

This work was supported by University of Tennessee, Center for Neurobiology of Brain Diseases and University of Tennessee, Center for Genomics and Bioinformatics (to R.H.); The National Institutes of Health RR 10522, RR 14593, and the National Science Foundation DBI 9604633 (to D.M.D.); and The Swiss Society for Research on Muscle Diseases and the Swiss Natl. Science Foundation grant Nr. 3100/0-/02075/1 (to T.W). We thank members of Homayouni laboratory for helpful discussions.

#### Appendix A. Supplementary data

Supplementary data associated with this article can be found, in the online version, at doi:10.1016/j.mcn.2005.09.015.

#### References

- Anandatheerthavarada, H.K., Biswas, G., Robin, M.A., Avadhani, N.G., 2003. Mitochondrial targeting and a novel transmembrane arrest of Alzheimer's amyloid precursor protein impairs mitochondrial function in neuronal cells. *J. Cell Biol.* 161, 41–54.
- Bonifacino, J.S., Traub, L.M., 2003. Signals for sorting of transmembrane proteins to endosomes and lysosomes. *Annu. Rev. Biochem.* 72, 395–447.
- D'Arcangelo, G., Homayouni, R., Keshvara, L., Rice, D.S., Sheldon, M., Curran, T., 1999. Reelin is a ligand for lipoprotein receptors. *Neuron* 24, 471–479.
- De Strooper, B., Annaert, W., 2000. Proteolytic processing and cell biological functions of the amyloid precursor protein. *J. Cell Sci.* 113 (Pt. 11), 1857–1870.
- Dolder, M., Wendt, S., Wallimann, T., 2001. Mitochondrial creatine kinase in contact sites: interaction with porin and adenine nucleotide translocase, role in permeability transition and sensitivity to oxidative damage. *Biol. Signals Recept.* 10, 93–111.
- Dolder, M., Walzel, B., Speer, O., Schlattner, U., Wallimann, T., 2003. Inhibition of the mitochondrial permeability transition by creatine kinase substrates. Requirement for microcompartmentation. *J. Biol. Chem.* 278, 17760–17766.
- Eckert, A., Keil, U., Marques, C.A., Bonert, A., Frey, C., Schussel, K., Muller, W.E., 2003. Mitochondrial dysfunction, apoptotic cell death, and Alzheimer's disease. *Biochem. Pharmacol.* 66, 1627–1634.
- Eggert, S., Paliga, K., Soba, P., Evin, G., Masters, C.L., Weidemann, A., Beyreuther, K., 2004. The proteolytic processing of the amyloid precursor protein gene family members APLP-1 and APLP-2 involves alpha-, beta-, gamma-, and epsilon-like cleavages: modulation of APLP-1 processing by n-glycosylation. *J. Biol. Chem.* 279, 18146–18156.
- Galvan, V., Chen, S., Lu, D., Logvinova, A., Goldsmith, P., Koo, E.H., Bredesen, D.E., 2002. Caspase cleavage of members of the amyloid precursor family of proteins. *J. Neurochem.* 82, 283–294.
- Gibson, G.E., Sheu, K.F., Blass, J.P., 1998. Abnormalities of mitochondrial enzymes in Alzheimer disease. *J. Neural Transm.* 105, 855–870.
- Hall, E.D., Oostveen, J.A., Dunn, E., Carter, D.B., 1995. Increased amyloid protein precursor and apolipoprotein E immunoreactivity in the selectively vulnerable hippocampus following transient forebrain ischemia in gerbils. *Exp. Neurol.* 135, 17–27.
- Hatano, E., Tanaka, A., Kanazawa, A., Tsuyuki, S., Tsunekawa, S., Iwata, S., Takahashi, R., Chance, B., Yamaoka, Y., 2004. Inhibition of tumor necrosis factor-induced apoptosis in transgenic mouse liver expressing creatine kinase. *Liver Int.* 24, 384–393.
- Heber, S., Herms, J., Gajic, V., Hainfellner, J., Aguzzi, A., Rulicke, T., von Kretschmar, H., von Koch, C., Sisodia, S., Tremml, P., Lipp, H.P., Wolfner, D.P., Muller, U., 2000. Mice with combined gene knock-outs reveal essential and partially redundant functions of amyloid precursor protein family members. *J. Neurosci.* 20, 7951–7963.
- Ho, A., Sudhof, T.C., 2004. Binding of F-spondin to amyloid-beta precursor protein: a candidate amyloid-beta precursor protein ligand that modulates amyloid-beta precursor protein cleavage. *Proc. Natl. Acad. Sci. U. S. A.* 101, 2548–2553.
- Homayouni, R., Rice, D.S., Sheldon, M., Curran, T., 1999. Disabled-1 binds to the cytoplasmic domain of amyloid precursor-like protein 1. *J. Neurosci.* 19, 7507–7515.
- Homayouni, R., Rice, D.S., Curran, T., 2001. Disabled-1 interacts with a novel developmentally regulated protocadherin. *Biochem. Biophys. Res. Commun.* 289, 539–547.
- Joubert, F., Mazet, J.L., Mateo, P., Hoerter, J.A., 2002. 31P NMR detection of subcellular creatine kinase fluxes in the perfused rat heart: contractility modifies energy transfer pathways. *J. Biol. Chem.* 277, 18469–18476.
- Kamal, A., Stokin, G.B., Yang, Z., Xia, C.H., Goldstein, L.S., 2000. Axonal transport of amyloid precursor protein is mediated by direct binding to the kinesin light chain subunit of kinesin-I. *Neuron* 28, 449–459.
- Kamal, A., Almenar-Queralt, A., LeBlanc, J.F., Roberts, E.A., Goldstein, L.S., 2001. Kinesin-mediated axonal transport of a membrane compartment containing beta-secretase and presenilin-1 requires APP. *Nature* 414, 643–648.
- Kanazawa, A., Tanaka, A., Iwata, S., Satoh, S., Hatano, E., Shinohara, H., Kitai, T., Tsunekawa, S., Ikai, I., Yamamoto, M., Takahashi, R., Chance, B., Yamaoka, Y., 1998. The beneficial effect of phosphocreatine accumulation in the creatine kinase transgenic mouse liver in endotoxin-induced hepatic cell death. *J. Surg. Res.* 80, 229–235.
- Kimberly, W.T., Zheng, J.B., Guenette, S.Y., Selkoe, D.J., 2001. The intracellular domain of the beta-amyloid precursor protein is stabilized by Fe65 and translocates to the nucleus in a notch-like manner. *J. Biol. Chem.* 276, 40288–40292.
- King, G.D., Scott Turner, R., 2004. Adaptor protein interactions: modulators of amyloid precursor protein metabolism and Alzheimer's disease risk? *Exp. Neurol.* 185, 208–219.
- King, G.D., Perez, R.G., Steinhilb, M.L., Gaut, J.R., Turner, R.S., 2003. X11alpha modulates secretory and endocytic trafficking and metabolism of amyloid precursor protein: mutational analysis of the YENPTY sequence. *Neuroscience* 120, 143–154.
- Kogel, D., Schomburg, R., Schurmann, T., Reimertz, C., Konig, H.G.,

- Poppe, M., Eckert, A., Muller, W.E., Prehn, J.H., 2003. The amyloid precursor protein protects PC12 cells against endoplasmic reticulum stress-induced apoptosis. *J. Neurochem.* 87, 248–256.
- Liautaud, J.P., 1994. A hypothesis on the aetiology of Alzheimer's disease: description of a model involving a misfolded chaperone. *Med. Hypotheses* 43, 372–380.
- Lin, B., Schmidt-Kastner, R., Busto, R., Ginsberg, M.D., 1999. Progressive parenchymal deposition of beta-amyloid precursor protein in rat brain following global cerebral ischemia. *Acta Neuropathol. (Berl)* 97, 359–368.
- Lyckman, A.W., Confaloni, A.M., Thinakaran, G., Sisodia, S.S., Moya, K.L., 1998. Post-translational processing and turnover kinetics of presynaptically targeted amyloid precursor superfamily proteins in the central nervous system. *J. Biol. Chem.* 273, 11100–11106.
- Mattson, M.P., 1997. Mother's legacy: mitochondrial DNA mutations and Alzheimer's disease. *Trends Neurosci.* 20, 373–375.
- Mihara, K., Omura, T., 1996. Cytoplasmic chaperones in precursor targeting to mitochondria: the role of MSF and hsp 70. *Trends Cell Biol.* 6, 104–108.
- Nishimoto, I., Okamoto, T., Matsuura, Y., Takahashi, S., Murayama, Y., Ogata, E., 1993. Alzheimer amyloid protein precursor complexes with brain GTP-binding protein G(o). *Nature* 362, 75–79.
- O'Gorman, E., Beutner, G., Dolder, M., Koretsky, A.P., Brdiczka, D., Wallimann, T., 1997. The role of creatine kinase in inhibition of mitochondrial permeability transition. *FEBS Lett.* 414, 253–257.
- Pfanner, N., Wiedemann, N., 2002. Mitochondrial protein import: two membranes, three translocases. *Curr. Opin. Cell Biol.* 14, 400–411.
- Rapoport, S.I., Hatanpaa, K., Brady, D.R., Chandrasekaran, K., 1996. Brain energy metabolism, cognitive function and down-regulated oxidative phosphorylation in Alzheimer disease. *Neurodegeneration* 5, 473–476.
- Reddy, P.H., McWeeney, S., Park, B.S., Manczak, M., Gutala, R.V., Partovi, D., Jung, Y., Yau, V., Searles, R., Mori, M., Quinn, J., 2004. Gene expression profiles of transcripts in amyloid precursor protein transgenic mice: up-regulation of mitochondrial metabolism and apoptotic genes is an early cellular change in Alzheimer's disease. *Hum. Mol. Genet.* 13, 1225–1240.
- Scheinfeld, M.H., Ghersi, E., Laky, K., Fowlkes, B.J., D'Adamo, L., 2002. Processing of beta-amyloid precursor-like protein-1 and -2 by gamma-secretase regulates transcription. *J. Biol. Chem.* 277, 44195–44201.
- Schlattner, U., Forstner, M., Eder, M., Stachowiak, O., Fritz-Wolf, K., Wallimann, T., 1998. Functional aspects of the X-ray structure of mitochondrial creatine kinase: a molecular physiology approach. *Mol. Cell. Biochem.* 184, 125–140.
- Schlattner, U., Eder, M., Dolder, M., Khuchua, Z.A., Strauss, A.W., Wallimann, T., 2000. Divergent enzyme kinetics and structural properties of the two human mitochondrial creatine kinase isoenzymes. *Biol. Chem.* 381, 1063–1070.
- Schlattner, U., Dolder, M., Wallimann, T., Tokarska-Schlattner, M., 2001. Mitochondrial creatine kinase and mitochondrial outer membrane porin show a direct interaction that is modulated by calcium. *J. Biol. Chem.* 276, 48027–48030.
- Schlattner, U., Mockli, N., Speer, O., Werner, S., Wallimann, T., 2002. Creatine kinase and creatine transporter in normal, wounded, and diseased skin. *J. Invest. Dermatol.* 118, 416–423.
- Selkoe, D.J., 2000. Toward a comprehensive theory for Alzheimer's disease. Hypothesis: Alzheimer's disease is caused by the cerebral accumulation and cytotoxicity of amyloid beta-protein. *Ann. N. Y. Acad. Sci.* 924, 17–25.
- Smith, C.D., Carney, J.M., Starke-Reed, P.E., Oliver, C.N., Stadtman, E.R., Floyd, R.A., Markesbery, W.R., 1991. Excess brain protein oxidation and enzyme dysfunction in normal aging and in Alzheimer disease. *Proc. Natl. Acad. Sci. U. S. A.* 88, 10540–10543.
- Steinbach, J.P., Muller, U., Leist, M., Li, Z.W., Nicotera, P., Aguzzi, A., 1998. Hypersensitivity to seizures in beta-amyloid precursor protein deficient mice. *Cell Death Differ.* 5, 858–866.
- Streijger, F., Jost, C.R., Oerlemans, F., Ellenbroek, B.A., Cools, A.R., Wieringa, B., Van der Zee, C.E., 2004. Mice lacking the UbCKmit isoform of creatine kinase reveal slower spatial learning acquisition, diminished exploration and habituation, and reduced acoustic startle reflex responses. *Mol. Cell. Biochem.* 256–257, 305–318.
- Swerdlow, R.H., Khan, S.M., 2004. A "mitochondrial cascade hypothesis" for sporadic Alzheimer's disease. *Med. Hypotheses* 63, 8–20.
- Turner, P.R., O'Connor, K., Tate, W.P., Abraham, W.C., 2003. Roles of amyloid precursor protein and its fragments in regulating neural activity, plasticity and memory. *Prog. Neurobiol.* 70, 1–32.
- von Koch, C.S., Zheng, H., Chen, H., Trumbauer, M., Thinakaran, G., van der Ploeg, L.H., Price, D.L., Sisodia, S.S., 1997. Generation of APLP2 KO mice and early postnatal lethality in APLP2/APP double KO mice. *Neurobiol. Aging* 18, 661–669.
- Wallimann, T., Wyss, M., Brdiczka, D., Nicolay, K., Eppenberger, H.M., 1992. Intracellular compartmentation, structure and function of creatine kinase isoenzymes in tissues with high and fluctuating energy demands: the 'phosphocreatine circuit' for cellular energy homeostasis. *Biochem. J.* 281 (Pt. 1), 21–40.
- Wallimann, T., Dolder, M., Schlattner, U., Eder, M., Hornemann, T., O'Gorman, E., Ruck, A., Brdiczka, D., 1998. Some new aspects of creatine kinase (CK): compartmentation, structure, function and regulation for cellular and mitochondrial bioenergetics and physiology. *BioFactors* 8, 229–234.
- Wendt, S., Schlattner, U., Wallimann, T., 2003. Differential effects of peroxynitrite on human mitochondrial creatine kinase isoenzymes. Inactivation, octamer destabilization, and identification of involved residues. *J. Biol. Chem.* 278, 1125–1130.
- Yano, M., Kanazawa, M., Terada, K., Takeya, M., Hoogenraad, N., Mori, M., 1998. Functional analysis of human mitochondrial receptor Tom20 for protein import into mitochondria. *J. Biol. Chem.* 273, 26844–26851.
- Yano, M., Terada, K., Mori, M., 2003. AIP is a mitochondrial import mediator that binds to both import receptor Tom20 and preproteins. *J. Cell Biol.* 163, 45–56.
- Yuan, X., Desiderio, D.M., 2003. Proteomics analysis of phosphotyrosyl-proteins in human lumbar cerebrospinal fluid. *J. Proteome Res.* 2, 476–487.
- Yuan, X., Russell, T., Wood, G., Desiderio, D.M., 2002. Analysis of the human lumbar cerebrospinal fluid proteome. *Electrophoresis* 23, 1185–1196.
- Zheng, H., Jiang, M., Trumbauer, M.E., Sirinathsinghji, D.J., Hopkins, R., Smith, D.W., Heavens, R.P., Dawson, G.R., Boyce, S., Conner, M.W., et al., 1995. beta-Amyloid precursor protein-deficient mice show reactive gliosis and decreased locomotor activity. *Cell* 81, 525–531.
- Zheng, P., Eastman, J., Vande Pol, S., Pimplikar, S.W., 1998. PAT1, a microtubule-interacting protein, recognizes the basolateral sorting signal of amyloid precursor protein. *Proc. Natl. Acad. Sci. U. S. A.* 95, 14745–14750.
- Zhou, D., Novello, C., D'Ambrosio, C., Scaloni, A., D'Adamo, L., 2004. Growth factor receptor-bound protein 2 interaction with the tyrosine-phosphorylated tail of amyloid beta precursor protein is mediated by its Src homology 2 domain. *J. Biol. Chem.* 279, 25374–25380.